Experimental study on convective heat transfer of nanofluids in turbulent flow: Methods of comparison of their performance

Haghighi, Ehsan B.; Utomo, Adi T.; Ghanbarpour, Morteza; Izadi Tabaei Zavareh, Ashkan; Poth, Heiko; Khodabandeh, Rahmatollah; Pacek, Andrzej; Palm, Björn E.

DOI:
10.1016/j.expthermflusci.2014.05.019

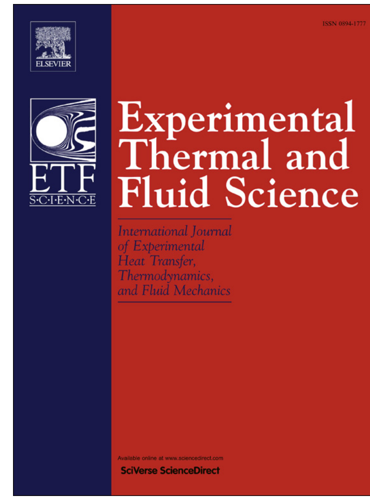

Experimental Study on Convective Heat Transfer of Nanofluids in Turbulent Flow: Methods of Comparison of Their Performance

Ehsan B. Haghighi, Adi T. Utomo, Morteza Ghanbarpour, Ashkan I.T. Zavareh, Heiko Poth, Rahmatollah Khodabandeh, Andrzej Pacek, Björn E. Palm

PII: S0894-1777(14)00140-X
DOI: http://dx.doi.org/10.1016/j.expthermflusci.2014.05.019
Reference: ETF 8235

To appear in: *Experimental Thermal and Fluid Science*

Received Date: 12 April 2014
Revised Date: 31 May 2014
Accepted Date: 31 May 2014

Please cite this article as: E.B. Haghighi, A.T. Utomo, M. Ghanbarpour, A.I.T. Zavareh, H. Poth, R. Khodabandeh, A. Pacek, B.E. Palm, Experimental Study on Convective Heat Transfer of Nanofluids in Turbulent Flow: Methods of Comparison of Their Performance, *Experimental Thermal and Fluid Science* (2014), doi: http://dx.doi.org/10.1016/j.expthermflusci.2014.05.019

Experimental Study on Convective Heat Transfer of Nanofluids in Turbulent Flow: Methods of Comparison of Their Performance

Ehsan B. Haghighi [1], Adi T. Utomo[2], Morteza Ghanbarpour[1], Ashkan I. T. Zavareh[3], Heiko Poth[4], Rahmatollah Khodabandeh[1], Andrzej Pacek[3], Björn E. Palm[1]*

1: KTH Royal Institute of Technology, Department of Energy Technology, 100 44 Stockholm, Sweden

2: BHR Virtual PiE, The Fluid Engineering Centre, Cranfield, MK43 0AJ, UK

3: University of Birmingham, School of Chemical Engineering, B15 2TT, Birmingham, UK

4: ItN Nanovation AG, Untertuerkheimer Straße 25, 66117 Saarbrücken, Germany

* *Correspoding author*

Abstract

Turbulent convective heat transfer coefficients of 9 wt% Al_2O_3/water and TiO_2/water nanofluids inside a circular tube were investigated independently at the Royal Institute of Technology, KTH (Sweden) and at University of Birmingham (UK). The experimental data from both laboratories agreed very well and clearly show that Nusselt numbers are well correlated by the equations developed for single phase fluids with the thermophysical properties of nanofluid.

The heat transfer coefficients of nanofluids can be compared with those of the base fluids at the same Reynolds number or at the same pumping power. As the same Reynolds number requires higher flow rate of nanofluids therefore such comparison shows up to 15% increase in heat transfer coefficient. However, at equal pumping power, the heat transfer coefficient of Al_2O_3 nanofluid was practically the same as that of water while that of TiO_2 was about 10% lower. Comparing performance at equal Reynolds number is clearly misleading since the heat transfer coefficient can always be increased by increased pumping power, accordingly, the comparison between the fluids should be done at equal pumping power.

Keywords: nanofluids, convective heat transfer, turbulent, circular tube, Al_2O_3, TiO_2, pumping power

Introduction

In the last decade the convective heat transfer of nanofluids in the turbulent flow was very frequently investigated and according to Science Direct, there were about 1000 articles investigating thermal performance of nanofluids in 2013 alone. Whilst there is still luck of consensus among scientists whether nanofluids show unusual thermal properties majority of papers claim that the presence small amount of nanoparticles drastically increases thermal conductivity and heat transfer coefficients [1] [2] [3].

Duangthongsuk and Wongwises [4] experimentally investigated the heat transfer and pressure drop in turbulent flow of TiO_2/water nanofluids (0.2–2 vol% TiO_2) in a horizontal double tube counterflow heat exchanger. They compared heat transfer coefficients in nanofluids with those in the base liquid at the same Re numbers (between 3000 and 18000) and observed 20–32% enhancement at 1.0% volume fraction of nanoparticles. However as the concentration of nanoparticles was increased to 2 vol% a reduction of the heat transfer coefficients by 14% was observed compared to base liquid.

Fotukian and Nasr Esfahany [5] investigated turbulent convective heat transfer in diluted γ-Al_2O_3/water nanofluids ($Al_2O_3 < 0.2$ vol%) in turbulent flow in a circular tube. They showed that, at the same Re number, heat transfer coefficients and pressure drops of nanofluids were higher than of the base fluid. A maximum increase of heat transfer coefficients by 48% was observed at volume fraction of nanoparticles of 0.054% and at Reynolds number of 10000.

Zamzamian et al. [6] investigated the effect of nanoparticles concentration and operating temperature on turbulent heat transfer coefficients in Al_2O_3/Ethylene Glycol (EG) and CuO/EG nanofluids (nanoparticles concentration between 0.1 and 1 wt%) in a double pipe and in a plate heat exchangers and reported an increase of heat transfer coefficients with the increase of particle concentration and operating temperature. They reported 3–49% enhancement of the heat transfer coefficients in nanofluids at the same Reynolds number.

Suresh et al. [7] investigated the heat transfer coefficient and friction factor in Al_2O_3/water nanofluids (0.3%, 0.4% and 0.5% Al_2O_3) in a turbulent flow through a straight pipe fitted with spiral inserts. At all Reynolds numbers, they observed almost the same values of the friction factors for the nanofluids as for the base fluids, and reported 10–48% enhancement in the Nusselt number in nanofluids at the same Reynolds number.

Fotukian and Nasr Esfahany [8] reported enhancement of the heat transfer coefficients by 25% and 20% increase of pressure drop in a turbulent flow of diluted CuO/water nanofluids (solid concentration larger than 0.3% v/v) in a circular tube comparing with water at the same Re number. They also found that the enhancement of heat transfer coefficient at all investigated Reynolds number was practically independent of the concentration of nanoparticles.

Sajadi and Kazemi [9] measured turbulent heat transfer coefficient and pressure drop in TiO_2/water nanofluid (TiO_2 volume fraction < 0.25%) in a circular tube and reported approximately 22% enhancement of the heat transfer coefficient and 25% increase in the pressure drop at Re=5000.

Turbulent convective heat transfer of the suspensions of γ-Al_2O_3, TiO_2 and CuO nanoparticles in aqueous solutions of carboxymethyl cellulose were investigated by Hojjat et al. [10]. They reported that the convective heat transfer coefficients in the nanofluids were higher than those in the base fluid when compared at equal Peclet numbers (Pe=Re×Pr) and that the heat transfer coefficient increases with the increase of Peclet number and nanoparticles concentration.

On the other hand, when compared at the same average velocity, the heat transfer coefficients of nanofluids were lower than those of the base fluids [11], [12]. The early work from Pak and Cho [11] showed that the heat transfer coefficient of alumina/water was up to 75% higher than the base fluid at the same Reynolds number, but it was 12% lower at the same average velocity. They argued that since the viscosity of nanofluids was higher than that of the base fluid, the Reynolds numbers of the nanofluids were lower than that of water at the same average velocity and consequently the heat transfer coefficient was lower. The results of Pak and Cho [11] clearly indicated that the heat transfer coefficient enhancements of nanofluids depended on the method of comparing them with those of base fluids. Yu et al. [13] also reported the same conclusion.

Table 1 summarizes some works investigating turbulent heat transfer in nanofluids.

Table 1 – Heat transfer in nanofluids in turbulent flow.

Figure 1. Increase in heat transfer coefficient versus nanoparticles concentration compared at the same Re

Some of the reported enhancement of heat transfer coefficient (compared at the same Re) plotted against concentration of nanoparticles summarised in **Fig. 1** and clearly show that there is no correlation between the two.

It is well known that there is no theory enabling explanation of unusual enhancement of thermal properties of nanofluids. Therefore in the great majority of the papers discussed above the experiments carried out by one research group are analysed and the results are presented as a graphs showing enhancement coefficients as a function of Re number or pumping power. In such a type of research there is very difficult, if possible at all, to verify experimental results.

In this paper we exploit the fact that the heat transfer in nanofluids was investigated in an EU sponsored project (NanoHex, Ref: 228882) by the consortium comprising universities, research establishment and companies. As it was already mentioned the bulk of experiments were carried out in B-ham and in Stockholm but all the results were heavily scrutinised by other members of the consortium during research meetings. This approach gives extra level of confidence as all the data presented in this paper were at least double/triple checked. Therefore the conclusions indicating that heat transfer coefficient in turbulent flow of nanofluid can be correlated by standard equations developed for ordinary fluids and that there is nothing unusual in thermal behaviour of nanofluids are sound.

Materials and Methods

Materials

The Al_2O_3 and TiO_2 nanofluids were supplied as concentrated suspensions (40 wt% for both) by ItN Nanovation AG (Germany) and Evonik AG (Germany), respectively. The concentrated suspensions were diluted to 9 wt% with distilled water (DW). **Fig. 2** shows the TEM micrographs of Al_2O_3 and TiO_2 nanoparticles and **Fig. 3** shows size distributions of nanoparticles/aggregates in the diluted suspension measured by dynamic light scattering (DLS). The physical properties of nanoparticles/nanofluids including pH, crystal phase, hydrodynamic particle size, average dry particle size (measured by TEM), and the concentration of additives (additives/surfactant) are summarized in **Table 2**.

Figure 2 - TEM micrographs of tested nanofluids (a) Al_2O_3, (b) TiO_2

Figure 3 - Size distribution of Al_2O_3 and TiO_2 nanoparticles measured by dynamic light scattering (DLS)

Table 2 Properties of investigated nanofluids

Thermal conductivity and viscosity

The thermal conductivity of the fluids was measured at KTH with a transient plane source (TPS) analyser (HotDisk model 2500) and with a transient hot wire (THW) analyser (KD2 Pro) at UBHAM. In both methods a sensor (No. 7577, TPS and KS-1, KD2 Pro) is immersed in the static liquid and thermal conductivity is calculated based on the analysis of transient temperature response to a low heat pulse. Moreover, a thermostat bath (accuracy better than ±0.01 ºC at KTH and ±0.1 ºC at UBHAM) was used in order to keep temperature equilibrium.

A coaxial cylinders' viscometer (Brookfield model DV-II+Pro with UL adapter) was used at KTH and a plate-cone rheometer (AR 1000, TA Instruments, US) was used at UBHAM to measure the viscosity of the fluids. The shear rate was varied in the range 0 – 160 1/s and 10 – 100 1/s on KTH and UBHAM instruments respectively and the samples were placed in a thermostat bath with accuracy better than ±0.1 ºC to maintain temperature equilibrium.

Experimental setup

Figure 4 - Experimental setup at (a) KTH and at (b) UBHAM

Two closed-loop experimental rigs, one at KTH, **Fig. 4a** and one at UBHAM, **Fig. 4b** were used to measure heat transfer coefficients in turbulent flow in a pipe. In both rigs the test sections consist of entrance region, ensuring that the flow was fully developed at the beginning of heating section where the wall temperatures were measured, and a mixing section ensuring uniform cross section temperature after the outlet of the test section. The test section in KTH was heated by Joule effect whereas in UBHAN a heating tape was closely wrapped around the outer surface of the pipe (For details see [18]). Several thermocouples measured wall temperatures along the pipe as well as temperatures in the fluid at the inlet and the outlet. Furthermore, both experimental rigs included a pump, a flow-meter, cooling bath to cool down the working fluid and to adjust the temperature at the inlet of the test section. The necessary amount of fluid in the rig at KTH was 250-280 ml and 500 ml in the UBHAM rig. In the KTH rig, the pressure drop in the test section, including the inlet section, was measured by a differential pressure transducer (GE Druck, PTX5060-TA-A3-CC-H0-PA, UK). Data acquisition systems were used to collect and to transfer the data (temperatures, pressure difference, mass flow rates and densities) to a computer. At steady state, data was recorded every three seconds for about five minutes and this procedure was repeated three times both at KTH and UBHAM. The highest standard deviations for the average of the three individual measurements were 5.5% and 3.6% for KTH and UBHAM, respectively. **Table 3** summarises key parameters for both experimental rigs.

Table 3 - Test loops parameters

Data reduction

The local convective heat transfer coefficients, h, the local Nusselt numbers, Nu, and the heat flux were calculated from:

$$h_x = \frac{q^{"}}{(T_w - T_f)} \tag{1}$$

$$Nu_x = \frac{h_x d}{k} \tag{2}$$

$$q^{"} = \frac{\dot{m} C_p (T_{out} - T_{in})}{A} \tag{3}$$

The average heat transfer coefficients were calculated as the area-weighted averages of the local heat transfer coefficients, and the average Nu numbers were calculated from the average heat transfer coefficients. The friction factor was calculated as:

$$f = \frac{\Delta P}{\rho u^2/2} \frac{d}{L} \tag{4}$$

Furthermore, the theoretical pumping power (without considering the mechanical and the electrical losses in the pump) was calculated as the product of pressure drop (Δp) and volume flow rate ($\dot{\forall}$):

$$P = \Delta p \times \dot{\forall} \tag{5}$$

Nusselt number was calculated from Gnielinski correlation [19]:

$$Nu = \frac{\left(\frac{f}{8}\right)(Re - 1000) Pr}{1 + 12.7 \left(\frac{f}{8}\right)^{0.5} (Pr^{0.66} - 1)} \left[1 + \left(\frac{d}{L}\right)^{\frac{2}{3}}\right] \left(\frac{Pr}{Pr_w}\right)^{0.11} \tag{6}$$

And f, from Filonenko correlation, [20]:

$$f = (1.82 \, log_{10} \, Re - 1.64)^{-2} \tag{7}$$

The density and specific heat of the nanofluids were calculated from:

$$\rho_{eff} = (1 - \phi_p) \rho_{bf} + \phi_p \rho_p \tag{8}$$

$$Cp_{eff} = \frac{\emptyset \rho_p Cp_p + (1 - \emptyset) \rho_f Cp_f}{\rho_{eff}} \tag{9}$$

Measured thermal conductivities of the nanofluids were compared with values calculated from Maxwell correlation for spherical particles [21]:

$$k_{eff} = \left[\frac{k_p + 2k_{bf} + 2(k_p - k_{bf})\emptyset}{k_p + 2k_{bf} - (k_p - k_{bf})\emptyset}\right] k_{bf} \tag{10}$$

Several models to calculate viscosity of nanofluids are suggested in the literature, but discrepancy in the results for similar materials [22] are significant. Therefore measured viscosities were used in calculating the Re and Pr numbers.

Uncertainty analysis

If z is a function of several independent variables, x_i, each with their own uncertainties, Δx_i, the overall uncertainty in z is calculated as [23]

$$\Delta z = \pm\sqrt{\sum_{i=1}^{n}\left(\frac{\partial f}{\partial x_i}\right)^2 (\Delta x_i)^2} \quad (11).$$

The expanded uncertainty is obtained by multiplying the overall uncertainty with the coverage factor ξ:

$$\Delta Z = \xi \Delta z \quad (12).$$

By assuming the uncertainty of independent parameters (**Table 4.a**) the maximum uncertainty of dependent parameters with 95% confidence ($\xi = 2$) for the friction factor and the pumping power and 99% confidence for the rest of variables ($\xi = 3$) can be calculated (**Table 4.b**). The errors of the independent parameters are equal or less than stated in the table in both rigs.

Table 4 - Uncertainty

Results and discussions

Thermal conductivity and viscosity

To validate the instruments, the thermal conductivity and viscosity of distilled water (DW) were measured at KTH and UBHAM and the results are compared in **Table 5** (reference values are also shown [24] [25]). There is very good agreement between the results obtained in KTH and UBHAM and the deviations are less than 2% for thermal conductivity and 4% for viscosity.

Measured thermal conductivity and viscosity of Al_2O_3 and TiO_2 nanofluids at 20 and 40˚C and thermal conductivity calculated from Maxwell equation are summarised in **Table 6**. The differences between thermal conductivities measured in KTH and in UBAHM and values calculated from Maxwell correlation are below 2% but viscosity differs by 5-12%.

KTH measurements show that the relative thermal conductivity (thermal conductivity of nanofluid to base fluid) and the relative viscosity (viscosity of nanofluid to base fluid) of Al_2O_3 nanofluids were 1.08 and 1.16 respectively and 1.07 and 1.24 for TiO_2 nanofluids. UBHAM measurements indicate that relative thermal conductivity and relative viscosity of Al_2O_3 nanofluids were 1.05 and 1.11 respectively and 1.05 and 1.22 for TiO_2. Slight differences in the treatment and preparation of the nanofluids at the two universities may have affected the state of agglomeration differently and are thought to be the reason for larger deviations compared to water, particularly concerning the viscosity.

Table 5 - Thermal conductivity and viscosity of distilled water at T=20˚C and 40˚C

Table 6 - Thermal conductivity and viscosity of nanofluids at T=20˚C (a) and T=40˚C (b)

Validation of convective heat transfer experimental setup

To validate the experimental setup, the experimental results for distilled water were compared to those predicted by Eq. (6). **Fig. 5a** and **Fig. 5b** show the comparison of the experimental data with the predicted ones at inlet temperatures of 25 ˚C and 40 ˚C, respectively. Most of experimental data agree with the predicted value within +/- 10% and only few data points show deviation larger than 10% but less than 20%. The experimental average Nusselt numbers were calculated from the local

Nusselt numbers with appropriate values of thermal conductivity and viscosity based on IAPWS [24] [25]. Theoretical Nusselt numbers were calculated using thermophysical properties at the average fluid temperature between inlet and outlet. An analysis of literature data showed that Eq. 6 predicts most of 800 experimental data points within ±20% [26].

Figure 5 - Comparison of experimental average Nusselt number with Gnielinski correlation (Eq. 6) for distilled water (DW): T_{inlet}=25 ˚C (a), T_{inlet}=40 ˚C (b)

Convective heat transfer coefficient of nanofluids

Fig. 6 and **Fig. 7** show the Nusselt numbers for Al_2O_3/water and TiO_2/water nanofluids, respectively, as a function of Reynolds number at two inlet temperatures 25 ˚C and 40 ˚C. The theoretical values in these figures were obtained from Eq. (6) with densities, specific heats, and thermal conductivities calculated from Eqs. (8), (9) and (10), respectively. Experimental viscosity values measured in KTH (**Table 6**) were used.

As shown in **Fig. 6,** the experimental data from KTH and UBHAM for Al_2O_3 nanofluid agree with the theoretical prediction within +/- 10%. At Reynolds numbers higher than 4000, the Nusselt numbers of Al_2O_3 nanofluid measured at KTH at higher inlet temperature (40 ˚C) are slightly higher than the predicted values with a maximum deviation of 19%. Most of UBHAM results, for the smaller range of Re, also fit well within +/- 10% of predictions. At the inlet temperature of 25 ˚C, the experimental data are slightly higher than the theoretical prediction, while at the inlet temperature of 40 ˚C, the experimental data are slightly lower than the theoretical prediction with a maximum deviation of less than 12%. **Fig. 7** reveals similar trends for the TiO_2 nanofluids. Most of experimental data from both KTH and UBHAM at both inlet temperatures agree with the theoretical prediction within +/- 10%. In all cases, the deviations from the theoretical value are less than 20%, which is similar to the accuracy correlations for single phase fluids [26].

These results show that the agreement with Eq. (6) is better at the lower inlet temperature for both nanofluids (**Fig. 6a** and **Fig. 7a**) and for DW (**Fig. 5a**) than at the higher temperature (**Fig. 5b, Fig. 6b** and **Fig. 7b**). In summary, the results showed that Eq. (6) predicts the Nusselt number for the tested nanofluids with accuracy better than 20% in the temperature range 25-40 ˚C.

Figure 6. Comparison between the experimental average Nusselt numbers and Nusselt numbers calculated from Eq. (6) for Al_2O_3 nanofluid at 25 ˚C (a) and 40 ˚C (b)

Figure 7. Comparison between the experimental average Nusselt numbers and Nusselt numbers calculated from Eq. (6) for TiO_2 nanofluid at 25 ˚C (a) and 40 ˚C (b)

Pressure drop

The "ideal" pumping power was calculated from the measured flow rate and the pressure drop over the KTH-test section. Friction factors were then calculated from the measured pressure drop and the results were compared with the Eq. (7). **Fig. 8** shows the friction factors as a function of Reynolds number for DW, TiO_2/Water and Al_2O_3/Water nanofluids at average temperatures in the range 25-55 ˚C. At Reynolds number higher than 4000 the friction factors calculated from the measured pressure drops are in a very good agreement with values predicted from Eq. (7) with a maximum deviation of

±10%. Again correlation developed for simple (single phase) fluids can be used to predict pressure drop for nanofluids if the correct thermophysical properties of the nanofluids are used.

Figure 8. Friction factors based on experimental results compared to the Eq. (7) [20]

Comparing convective heat transfer of nanofluids at equal Reynolds number and at equal pumping power

As mentioned in the introduction, the assessment of thermal performance of nanofluids depends on the basis used to compare the heat transfer coefficient of nanofluids with that of the base fluid [13]. **Fig. 9** and **Fig. 10** compare heat transfer coefficients at equal Reynolds numbers for Al_2O_3 and TiO_2 nanofluids with those of distilled water at 25 °C and 40 °C, whilst **Fig. 11** and **Fig. 12** compare the heat transfer coefficients for these nanofluids at equal pumping power. In all cases, Eq. (7) was used to calculate the theoretical values of the Nusselt numbers, and the increase in heat transfer of nanofluid compared to base fluid is shown in percent (**Fig. 9 – Fig. 12**).

It is clear that the heat transfer coefficients in the nanofluids at the same Reynolds number are higher than those in the base fluid in both KTH and UBHAM experiments (**Fig. 9** and **Fig. 10**). However, the experimental data from UBHAM show 4-8% enhancement of heat transfer coefficient whereas KTH data show 10-15% enhancement (see **Fig. 9** and **Fig. 10**).

The differences between measured and predicted heat transfer coefficients in nanofluids at equal pumping power, shown in **Fig. 11** and **Fig. 12,** are significantly lower than the differences at equal Reynolds number (**Fig. 9** and **Fig. 10)** in both KTH and UBHAM results. Furthermore, the theoretical predictions based on Eq. (7) show reduction of heat transfer coefficients of nanofluids, compared with that for distilled water at the same pumping power.

The predicted heat transfer coefficients in Al_2O_3 is lower than in TiO_2 nanofluids (**Fig. 9** and **Fig. 10**) what can be explained by higher viscosity for TiO_2 nanofluid therefore higher velocity to reach the same Reynolds number. On the other hand, when the basis of the comparison is the same pumping power (**Fig. 11** and **Fig. 12**) the predicted heat transfer coefficient for TiO_2 nanofluid is much lower since it has higher viscosity.

Obviously it is very important to use the appropriate method when comparing heat transfer performance of nanofluids to that of their base fluids. Thermal comparison of nanofluids and base fluids should take into account both heat transfer coefficient and pressure drop therefore comparison at equal pumping power is appropriate. Comparison at the same Reynolds number suggests that any fluid with higher viscosity has higher heat transfer coefficients and therefore is better as a coolant. Therefore, comparing heat transfer coefficients of nanofluids and base fluids at equal Reynolds number, although common in the literature, is misleading and such comparisons should be ignored.

From the theoretical point of view, a nanofluid will show thermal benefit over the base fluid at the same pumping power if the thermal conductivity enhancement is sufficiently higher than the increase in viscosity. However, most literature data [11], [12], [27], [17], [18] and also the data in this work, showed that the increases in viscosity of various nanofluids (Al_2O_3, TiO_2, SiC, ZrO_2) were higher than their thermal conductivity enhancements. The results of Buongiorno et al. [28] showed that the thermal conductivity of nanofluids can be predicted satisfactorily using the effective medium theory based model, i.e. Maxwell model. Based on this model, the thermal conductivity of nanofluids increases linearly with nanoparticle concentration:

$$\frac{k_{nf}}{k_{bf}} = 1 + 3\emptyset \quad (11)$$

Similarly, the Einstein correlation can be considered as the lower limit of viscosity increase:

$$\frac{\mu_{nf}}{\mu_{bf}} = 1 + 2.5\emptyset \quad (12)$$

However, most of literature data [22] showed that the viscosity of nanofluids increases non-linearly with nanoparticle concentration. Assuming the thermal conductivity and viscosity of nanofluids follows Eqs. (11) and (12), respectively, the maximum theoretical benefit of using nanofluids as a coolant in fully turbulent flow, instead of base fluid, for Al_2O_3 and TiO_2 nanofluids at the same pumping power in different volume concentrations is shown in **Fig. 13**. The advantage is very marginal and may not be sufficient in industrial applications considering the new problems of using nanofluid, such as sedimentation which may lead to blockage, erosion and corrosion of the cooling system.

Figure 9. Change in heat transfer coefficients for Al_2O_3 nanofluid at 25 ˚C (a) and 40 ˚C (b) compared to DW, at equal Re

Figure 10. Change in heat transfer coefficients for TiO_2 nanofluid at 25 ˚C (a) and 40 ˚C (b) compared to DW, at equal Re

Figure 11. Change in heat transfer coefficients for Al_2O_3 nanofluid at 25 ˚C (a) and 40 ˚C (b) compared to DW, at equal pumping power

Figure 12. Change in heat transfer coefficients for TiO_2 nanofluid at 25 ˚C and 40 ˚C compared to DW, at equal pumping power

Figure 13. Change in heat transfer coefficients for Al_2O_3 and TiO_2 nanofluids based on theoretical prediction at equal pumping power

Conclusions

Turbulent heat transfer in Al_2O_3/water and TiO_2/water nanofluids (9 wt% solid in both) in pipe circular tubes with constant heat flux at the walls was investigated experimentally at very similar conditions at KTH and UBHAM. It was found that when using the measured thermophysical properties of the nanofluids, correlations developed for simple fluids (Eq. 6 and Eq. 7) predict the Nusselt numbers and the friction factors in turbulent flow for all tested nanofluids within 20% and 10%, respectively. Therefore, from engineering point of view, both heat transfer and pressure drop of nanofluids can be predicted satisfactorily by using conventional correlations developed for single phase fluids.

The convective heat transfer coefficients of the nanofluids were compared with those of the base fluids at equal Reynolds number and at equal pumping power. Comparison at equal Reynolds number showed that the thermal performance of nanofluid with higher viscosity was better since higher volumetric flow rate was required to achieve the same Reynolds number. From a practical point of view, this is not a relevant comparison, as heat transfer can always be increased by increasing the flow rate. Although misleading, this method of comparison is still common in the literature [29], [30], [31], [32]. Evaluation of the heat transfer performance of the nanofluids at equal pumping power seems to be appropriate approach from industrial point of view as it takes into account the total cost to remove heat from the system, i.e. the pumping cost. Based on this criterion, both Al_2O_3 and TiO_2 nanofluids investigated in this work did not show any benefit for cooling applications in turbulent flow since the increases in viscosities were higher than the enhancements of heat transfer coefficient.

Acknowledgement
The financial support of the EU project NanoHex (Enhanced Nano-fluid Heat Exchange), Ref: 228882, for this study is highly appreciated.

Nomenclature

A	area, m^2
c_p	specific heat capacity, J/kgK
d	pipe diameter, m
DW	distilled water
EG	ethylene glycol
f	friction factor, -
h	heat transfer coefficient, W/m^2 K
k	thermal conductivity, W/m K
L	length, m
$\dot{m}$	mass flow rate, kg/s
Nu	Nusselt number, hd/k
Pe	Peclet number, $Re \times Pr$
Pr	Prandtl number, $(C_p\ \mu)/k$
Re	Reynolds number, $(\rho u d)/\mu$
Δp	pressure drop, Pa
q''	heat flux, W/m^2

P	pumping power, W
T	temperature, C
t	thickness, mm
u	velocity, m/s
x	axial distance, m
$\dot{\forall}$	volume flow rate, m^3/s
Greek letters	
ν	kinematic viscosity, m^2/s
ρ	density, kg/m^3
α	thermal diffusivity, m^2/s
∅	solid particle volume concentration, -
μ	dynamic viscosity, cP
Subscripts	
bf	base fluid
eff	effective
f	fluid
w	wall
in	inner
out	outer
p	nano particle
x	axial direction

References

[1] K. S. Hwang, S. P. Jang and S. U. S. Choi, "Flow and convective heat transfer characteristics of water-based Al2O3 nanofluids in fully developed laminar flow regime," Int J Heat Mass Transf, vol. 52, pp. 193-199, 2009.

[2] K. B. Anoop, T. Sundararajan and S. K. Das, "Effect of particle size on the convective heat transfer in nanofluid in the developing region," Int J Heat Mass Transf, vol. 52, pp. 2189-2195, 2009.

[3] D. Wen and Y. Ding, "Experimental investigation into convective heat transfer of nanofluids at the entrance region under laminar flow conditions," Int J Heat Mass Transf, vol. 47, pp. 5181-5188, 2004.

[4] W. Duangthongsuk and S. Wongwises, "An experimental study on the heat transfer performance and pressure drop of TiO2-water nanofluids flowing under a turbulent flow regime," Int J Heat Mass Transfer, vol. 53, p. 334–344, 2010.

[5] S. Fotukian and M. Nasr Esfahany, "Experimental investigation of turbulent convective heat transfer of dilute γ-Al2O3/water nanofluid inside a circular tube," Int J Heat Fluid Fl, vol. 31, p. 606–612, 2010.

[6] A. Zamzamian, S. N. Oskouie, A. Doosthoseini, A. Joneidi and M. Pazouki, "Experimental investigation of forced convective heat transfer coefficient in nanofluids of Al2O3/EG and CuO/EG in a double pipe and plate heat exchangers under turbulent flow," Exp Therm Fluid Sci, vol. 35, p. 495–502, 2011.

[7] S. Suresh, P. Selvakumar, M. Chandrasekar and V. Srinivasa Raman, "Experimental studies on heat transfer and friction factor characteristics of Al2O3/water nanofluid under turbulent flow with spiraled rod inserts," Chem Eng Process, vol. 53, p. 24–30, 2012.

[8] S. Fotukian and M. Nasr Esfahany, "Experimental study of turbulent convective heat transfer and pressure drop of dilute CuO/water nanofluid inside a circular tube," Int Commun Heat Mass, vol. 37, p. 214–219, 2010.

[9] A. Sajadi and M. Kazemi, "Investigation of turbulent convective heat transfer and pressure drop of TiO2/water nanofluid in circular tube," Int Commun Heat Mass, vol. 38, p. 1474–1478, 2011.

[10] M. Hojjat, S. G. Etemad, R. Bagheri and J. Thibault, "Turbulent forced convection heat transfer of non-Newtonian nanofluids," Exp Therm Fluid Sci, vol. 35, p. 1351–1356, 2011.

[11] B. Pak and Y. Cho, "Hydrodynamic and heat transfer study of dispersed fluids with submicron metallic oxide particles," Exp Heat Transfer, vol. 11, pp. 151-170, 1998.

[12] W. Yu, D. M. France, D. S. Smith, D. Singh, E. V. Timofeeva and J. L. Routbort, "Heat transfer to a silicon carbide/water nanofluid," Int J Heat Mass Transferr, vol. 52, p. 3606–3612, 2009.

[13] W. Yu, D. M. France, E. V. Timofeeva, D. Singh and J. L. Routbort, "Thermophysical property-related comparison criteria for nanofluid heat transfer enhancement in turbulent flow," Appl Phys Lett, vol. 96, p. 213109 (3 pp.), 2010.

[14] Y. He, Y. Jin, H. Chen, Y. Ding, D. Cang and H. Lu, "Heat transfer and flow behavior of aqueous suspensions of TiO2 nanoparticles (nanofluids) flowing upward through a vertical pipe," Int J Heat Mass Transf, vol. 50, p. 2272–2281, 2007.

[15] D. Kulkarni, P. Namburu, H. Bargar and D. Das, "Convective heat transfer and fluid dynamic characteristics of SiO2-ethylene glycol/water nanofluid," Heat Transfer Eng, vol. 29, p. 1027–1035, 2008.

[16] M. H. Kayhani, H. Soltanzadeh, M. M. Heyhat, M. Nazari and F. Kowsary, "Experimental study of convective heat transfer and pressure drop of TiO2/water nanofluid," Int Commun Heat Mass, vol. 39, p. 456–462, 2012.

[17] E. B. Haghighi, M. Saleemi, N. Nikkam, R. Khodabandeh, M. S. Toprak, M. Muhammed and B. Palm, "Accurate basis of comparison for convective heat transfer in nanofluids," Int. Commun. Heat Mass, vol. 52, pp. 1-7, 2014.

[18] A. T. Utomo, H. Poth, P. T. Robbins and A. W. Pacek, "Experimental and theoretical studies of thermal conductivity, viscosity and heat transfer coefficient of titania and alumina nanofluids," Int J Heat Mass Transfer, vol. 55, p. 7772–7781, 2012.

[19] V. Gnielinski, "New Correlations for Heat and Mass Transfer in Turbulent Pipe and Channel Flow," Forsch Ingenieurwes, vol. 41, pp. 8-16, 1975.

[20] B. V. Karlekar and R. M. Desmond, Engineering Heat Transfer, West Publishing Company, 1977.

[21] J. C. Maxwell, A treatise on electricity and magnetism, Oxford: Clarendon Press, 1873.

[22] Mahbubul, I.M.; Saidur, R.; Amalina, M.A., "Latest developments on the viscosity of nanofluids," Int. J. Heat Mass Transf., vol. 55, pp. 874-885, 2011.

[23] J. Andraos, "On the propagation of statistical errors for a function of several variables," Journal of Chemical Education, vol. 73, no. 2, p. 150, 1996.

[24] "Release on the IAPWS Formulation 2011 for the Thermal Conductivity of Ordinary Water Substance (September 2011)," [Online]. Available: http://www.iapws.org. [Accessed 9 10 2012].

[25] "Release on the IAPWS Formulation 2008 for the Viscosity of Ordinary Water Substance (September 2008)," [Online]. Available: http://www.iapws.org.. [Accessed 9 10 2012].

[26] W. Ji, D. Zhang, Y. He and W. Tao, "Prediction of fully developed turbulent heat transfer of internal helically ribbed tubes – An extension of Gnielinski equation," Int J Heat Mass Transfer, vol. 55, p. 1375–1384, 2012.

[27] W. Williams, J. Buongiorno and L. Hu, "Experimental investigation of turbulent convective heat transfer and pressure loss of alumina/water and zirconia/water nanoparticle colloids (nanofluids) in horizontal tubes," J Heat Transfer, vol. 130, no. 4, p. 042412 (7 pages), 2008.

[28] Buongiorno, J. et al., "A benchmark study on the thermal conductivity of nanofluids," J. Appl. Phys., vol. 106, p. 094312, 2009.

[29] M. S. Mojarrad, A. Keshavarz, M. Ziabasharhagh and M. M. Raznahan, "Experimental investigation on heat transfer enhancement of alumina/water and alumina/water–ethylene glycol nanofluids in thermally developing laminar flow," Exp Therm Fluid Sci, vol. 53, p. 111–118, 2014.

[30] B. Abreu, B. Lamas, A. Fonseca, N. Martins and M. S. A. Oliveira, "Experimental characterization of convective heat transfer with MWCNT based nanofluids under laminar flow conditions," Heat Mass Transf., vol. 50, p. 65–74, 2014.

[31] L. S. Sundar, M. K. Singh, I. Bidkin and A. C. M. Sousa, "Experimental investigations in heat transfer and friction factor of magnetic Ni nanofluid flowing in a tube," Int. J. Heat Mass Transfer, vol. 70, p. 224–234, 2014.

[32] Ebrahimi, M.; Farhadi, M.; Sedighi, K.; Akbarzade, S., "Experimental investigation of force convection heat transfer in a car radiator filled with SiO2-water nanofluid," IJE, vol. 27, pp. 333-340, 2014.

Equation

$$h_x = \frac{q^{"}}{(T_w - T_f)} \tag{1}$$

$$Nu_x = \frac{h_x d}{k} \tag{2}$$

$$q^{"} = \frac{\dot{m} C_p (T_{out} - T_{in})}{A} \tag{3}$$

$$f = \frac{\Delta P}{\rho u^2/2} \frac{d}{L} \tag{4}$$

$$P = \Delta p \times \dot{\forall} \tag{5}$$

$$Nu = \frac{\left(\frac{f}{8}\right)(Re - 1000) Pr}{1 + 12.7 \left(\frac{f}{8}\right)^{0.5} (Pr^{0.66} - 1)} \left[1 + \left(\frac{d}{L}\right)^{\frac{2}{3}}\right] \left(\frac{Pr}{Pr_w}\right)^{0.11} \tag{6}$$

$$f = (1.82 \, log_{10} \, Re - 1.64)^{-2} \tag{7}$$

$$\rho_{eff} = (1 - \phi)\rho_{bf} + \phi \rho_p \tag{8}$$

$$Cp_{eff} = \frac{\emptyset \rho_p Cp_p + (1 - \emptyset) \rho_f Cp_f}{\rho_{eff}} \tag{9}$$

$$k_{eff} = \left[\frac{k_p + 2k_{bf} + 2(k_p - k_{bf})\emptyset}{k_p + 2k_{bf} - (k_p - k_{bf})\emptyset}\right] k_{bf} \tag{10}$$

$$\Delta z = \pm \sqrt{\sum_{i=1}^{n} \left(\frac{\partial f}{\partial x_i}\right)^2 (\Delta x_i)^2} \tag{11}$$

$$\Delta Z = \xi \Delta z \tag{12}$$

Author	**Nanofluid**	**Dimension, *Re***	**Basis of Comparison**	**Enhancement of h_{nf} and comments**
Pak and Cho (1998) [11]	γ-Al_2O_3/water and TiO_2/water 1–3 vol%	D=10.66 mm, L=4800 mm, Re=10^4–10^5	Same velocity	12% lower for γ-Al_2O_3/water at 3 vol %
He et al. (2007) [14]	TiO_2/water 0.2–1.1 vol%	D=3.97 mm, L=1834 mm, Re=2000–6000	Same *Re*	Maximum 40% enhancement for 1.1 vol % at Re=5900
Kulkarni (2008) [15]	TiO_2/(EG–water 60:40 wt%) 2–10 vol%	D=3.14 mm, L=1000 mm, Re=3000–12000	Same Re	16% enhancement for 10 vol % at Re=10000
Yu et al. (2009) [12]	SiC/water 3.7 vol%	D=2.27 mm, L=580 mm, Re=3300–13000	Same velocity	7% lower
Duangthongsuk and Wongwises (2010) [4]	TiO_2/water 0.2–2.0 vol%	D=9.53 mm, L=1500 mm, Re=3000–18000	Same *Re*	20-32% enhancement at 1.0 vol %
Fotukian and Nasr Esfahany (2010) [8]	CuO/water less than 0.24 vol%	D=5 mm, L=1000 mm, Re=6000-31000	Same *Re*	Maximum 25% enhancement
Fotukian and Nasr Esfahany (2010) [5]	γ-Al_2O_3/water less than 0.2 vol%	D=5 mm, L=1000 mm, Re=6000-31000	Same *Re*	48% enhancement at Re= 10000 and 0.054 vol%
Sajadi and Kazemi (2011) [9]	TiO_2/water less than 0.25 vol%.	D=5 mm, L=1800 mm, Re=5000-30000	Same *Re*	~22% enhancement at Re=5000 and 0.25 vol%
Suresh et al. (2012) [7]	Al_2O_3/water 0.3-0.5 vol%	D=4.85 mm, L=800 mm, Re=700-2050	Same *Re*	10-48% enhancement
Kayhani et al. (2012) [16]	TiO_2/water 0.1-2.0 vol%	D=5 mm, L=2000 mm, Re=6000-16000	Same *Re*	8% enhancement at Re= 11800 and 2.0 vol%
Haghighi et al. (2014) [17]	Al_2O_3, TiO_2, ZrO_2/water 9 wt%	D=3.7 mm, L=1500 mm, Re=2000-10000	Same pumping power	63%, 17%, and 52% lower for Al_2O_3, TiO_2, ZrO_2 respectively

Nanofluids	pH	Crystal phase	Primary particle size (TEM) (nm)	Most common aggregate particle size (DLS) (nm)	g Additives per g solid
Alumina ItN Nanovation	9.1	α	100-200	200	0.018
Titania Evonik (Aerodisp W740X)	6.7	85% anatase, 15% rutile	15 – 50	120	0.03

Parameters	KTH	UBHAM
Pipe (material, d_{in}, and t)	SS, 3.70 mm, 1.5 mm	SS, 4.57 mm, 0.89 mm
Entrance, heating, and mixing sections	250 mm, 1468 mm, 80 mm	650 mm, 1220 mm, 100 mm
Temperature recording: wall, inlet, outlet	All with thermocouples: 16 T-type (0.6 × 1.0 mm) for the wall, 2 and 3 T-type (0.5 mm) for the inlet and the outlet respectively	9 T-type (0.08 mm) thermocouples for the wall, 2 Pt 100 RTD (3 mm) for the inlet and the outlet
Accuracy of temperature measurement	Better than 0.1˚C	0.03˚C at 0˚C for the Pt 100 RTD and 0.1˚C for the thermocouples
Type of heater and power	Direct electric current (DC), 3000 W	Electric rope heater, 300 W
Type of insulation and heat loss from the system	Armaflex foam (with k ≤ 0.036 W/mK) and fiber glass insulation (with k = 0.035W/mK), less than 5%	Phenolic foam insulator (with k=0.02W/mK), less than 5%
Pump	Gear pump (MCP-Z, Ismatec, Switzerland) with pump head (170-000, Micropump, USA)	Peristaltic pump (Watson-Marlow 520, UK)
Flow-meter	Coriolis mass flow meter (CMFS015 with 2700 transmitter, Micromotion, Netherlands)	Coriolis mass flow meter (Optimas 3000-S3, Krohne, UK)
Cooling jacket	1.7m double pipe and a plate heat exchangers, plus small chiller (180 W cooling capacity)	2m double-pipe heat exchanger, chiller (400 W cooling capacity)

(a)

Independent parameters	Uncertainty
L	± 1 mm
D	± 0.01 mm
k	2%
μ	4%
ρ	1%
Cp	1%
T	± 0.1 ºC
m	0.1%
ΔP	± 0.0054 bar

(b)

Dependent parameters	Uncertainty (%)
f	10*
P	10*
Re	11
h, average	9
Nu, average	11

*** For 70% of experimental data.**

	k ($Wm^{-1}K^{-1}$)			μ (cP)		
T (˚C)	**Ref.**	**KTH**	**UBHAM**	**Ref.**	**KTH**	**UBHAM**
20	0.599	0.590	0.594	1.002	1.033	0.974
40	0.631	0.633	-	0.653	0.679	0.668

T=20°C	k ($Wm^{-1}K^{-1}$)			μ (cP)	
Material	**KTH**	**UBHAM**	**Maxwell**	**KTH**	**UBHAM**
Al_2O_3	0.642	0.638	0.641	1.225	1.074
TiO_2	0.636	0.626	0.636	1.315	1.152

(a)

T=40°C	k ($Wm^{-1}K^{-1}$)			μ (cP)	
Material	**KTH**	**UBHAM**	**Maxwell**	**KTH**	**UBHAM**
Al_2O_3	0.688	-	0.675	0.804	0.741
TiO_2	0.672	-	0.670	0.865	0.821

(b)

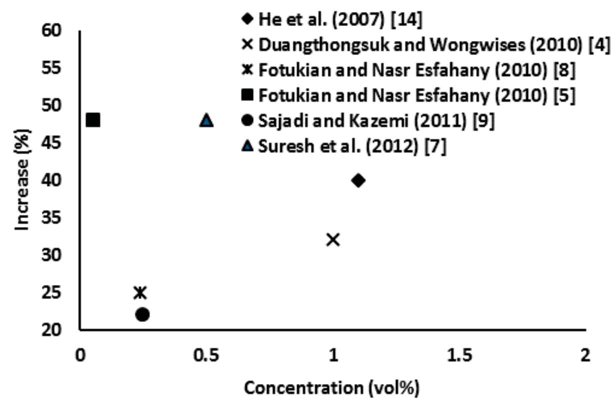
He et al. (2007) [14]
Duangthongsuk and Wongwises (2010) [4]
Fotukian and Nasr Esfahany (2010) [8]
Fotukian and Nasr Esfahany (2010) [5]
Sajadi and Kazemi (2011) [9]
Suresh et al. (2012) [7]
Increase (%)
Concentration (vol%)
60
55
50
45
40
35
30
25
20
0
0.5
1
1.5
2

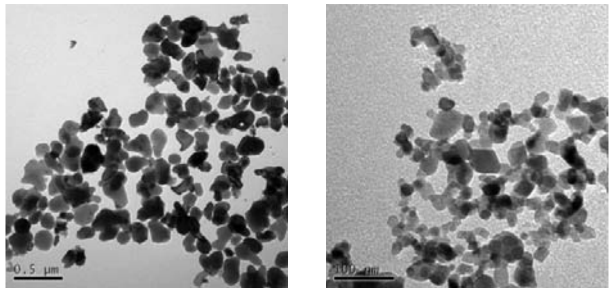

(a) (b)

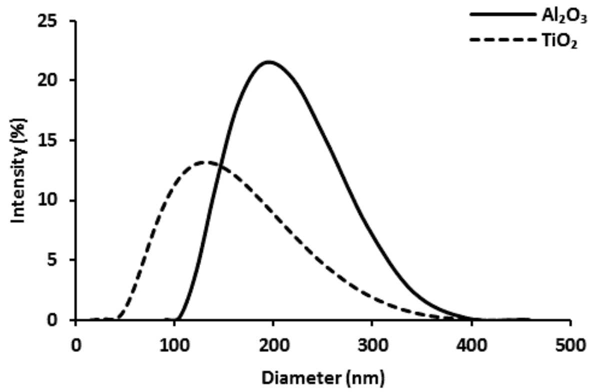

Al2O3
TiO2
Intensity (%)
25
20
15
10
5
0
0
100
200
300
400
500
Diameter (nm)

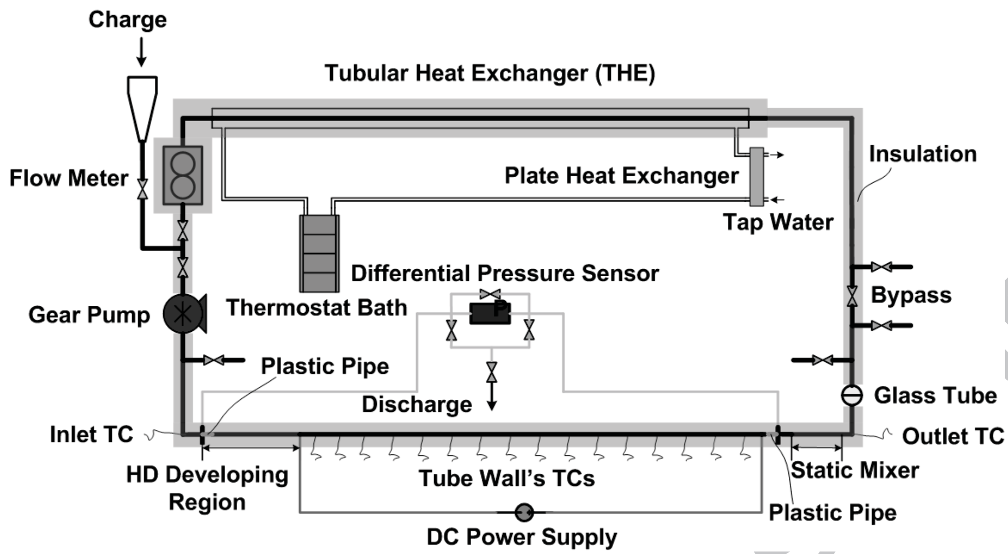

Charge
Tubular Heat Exchanger (THE)
Flow Meter
Plate Heat Exchanger
Insulation
Tap Water
Differential Pressure Sensor
Gear Pump
Thermostat Bath
Bypass
Plastic Pipe
Discharge
Glass Tube
Inlet TC
Outlet TC
HD Developing Region
Tube Wall's TCs
Static Mixer
Plastic Pipe
DC Power Supply

(a)

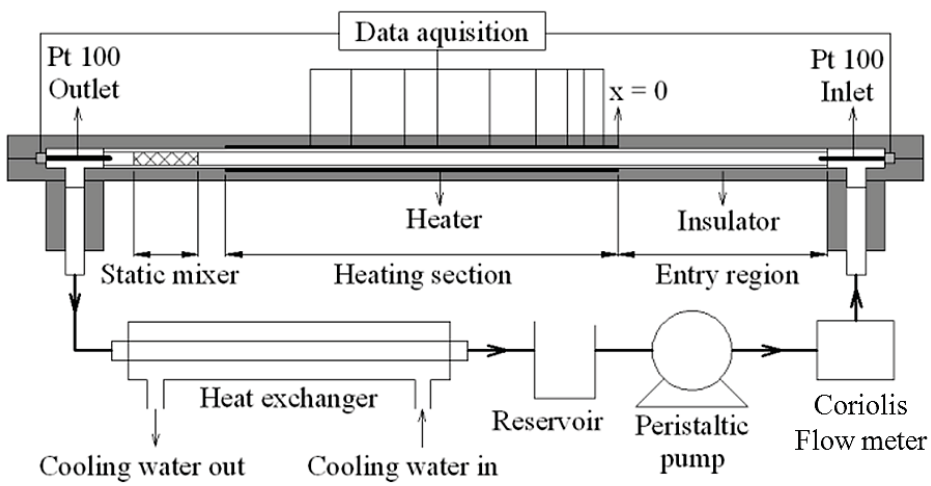

Data aquisition
Pt 100 Outlet
x = 0
Pt 100 Inlet
Heater
Insulator
Static mixer
Heating section
Entry region
Heat exchanger
Reservoir
Peristaltic pump
Coriolis Flow meter
Cooling water out
Cooling water in

(b)

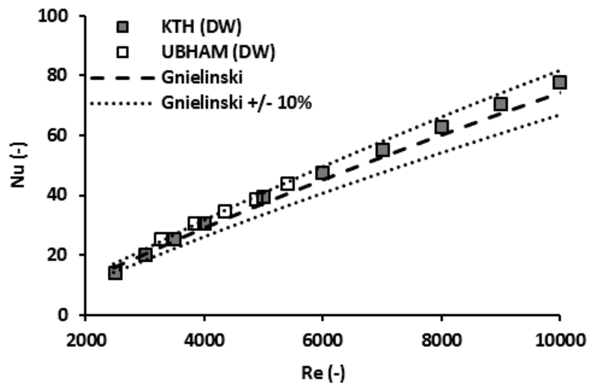
100
80
60
40
20
0
2000
4000
6000
8000
10000
Nu (-)
Re (-)
KTH (DW)
UBHAM (DW)
Gnielinski
Gnielinski +/- 10%

(a)

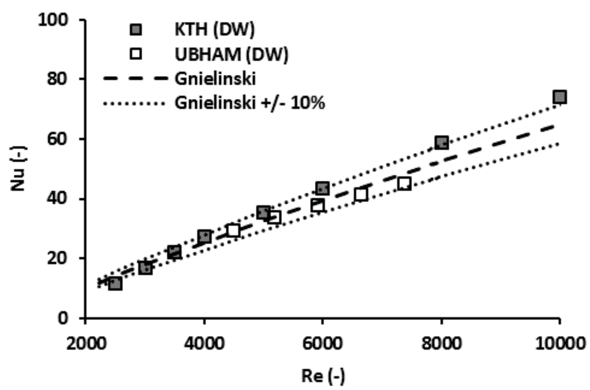
100
80
60
40
20
0
2000
4000
6000
8000
10000
Nu (-)
Re (-)
KTH (DW)
UBHAM (DW)
Gnielinski
Gnielinski +/- 10%

(b)

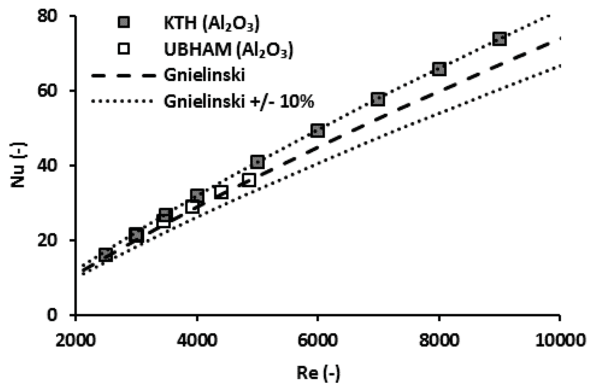

KTH (Al_2O_3)
UBHAM (Al_2O_3)
Gnielinski
Gnielinski +/- 10%
Nu (-)
Re (-)
0
20
40
60
80
2000
4000
6000
8000
10000

(a)

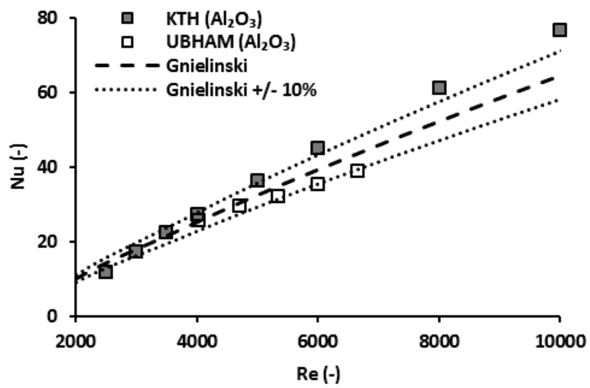

KTH (Al_2O_3)
UBHAM (Al_2O_3)
Gnielinski
Gnielinski +/- 10%
Nu (-)
Re (-)
0
20
40
60
80
2000
4000
6000
8000
10000

(b)

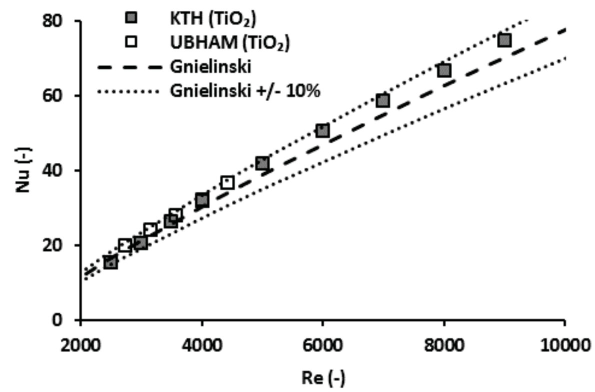
KTH (TiO_2)
UBHAM (TiO_2)
Gnielinski
Gnielinski +/- 10%
Nu (-)
Re (-)
0
20
40
60
80
2000
4000
6000
8000
10000

(a)

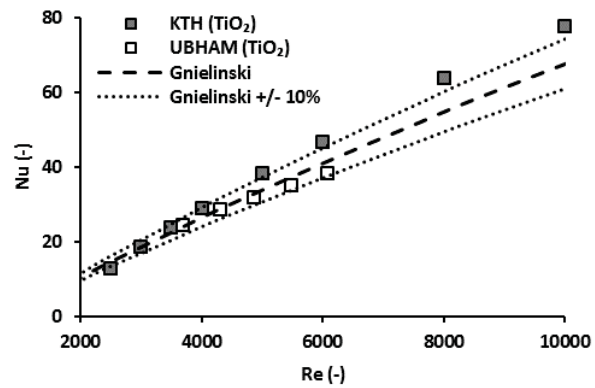
KTH (TiO_2)
UBHAM (TiO_2)
Gnielinski
Gnielinski +/- 10%
Nu (-)
Re (-)
0
20
40
60
80
2000
4000
6000
8000
10000

(b)

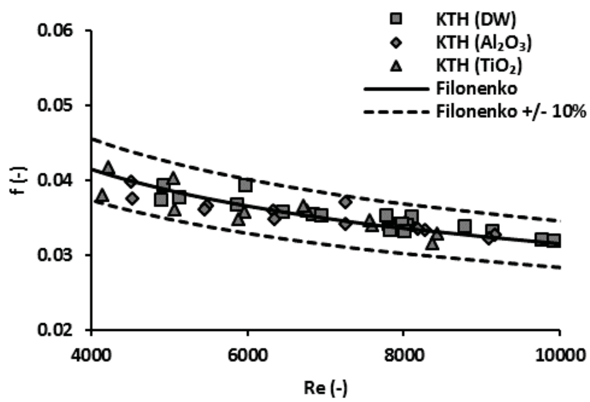
KTH (DW)
KTH (Al2O3)
KTH (TiO2)
Filonenko
Filonenko +/- 10%
0.06
0.05
0.04
0.03
0.02
f (-)
4000
6000
8000
10000
Re (-)

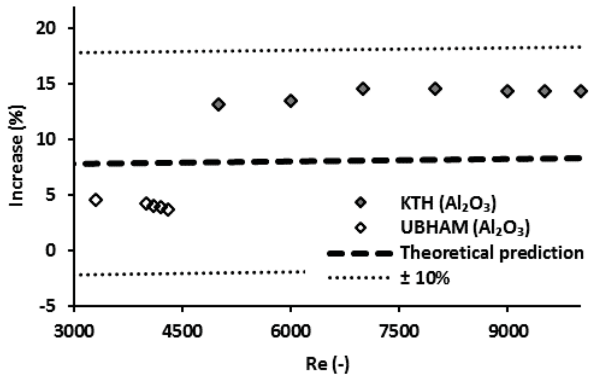

20
15
10
5
0
-5
Increase (%)
3000
4500
6000
7500
9000
Re (-)
KTH (Al_2O_3)
UBHAM (Al_2O_3)
Theoretical prediction
± 10%

(a)

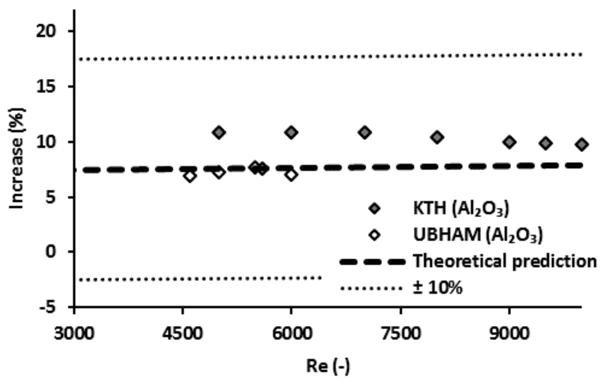

20
15
10
5
0
-5
Increase (%)
3000
4500
6000
7500
9000
Re (-)
KTH (Al_2O_3)
UBHAM (Al_2O_3)
Theoretical prediction
± 10%

(b)

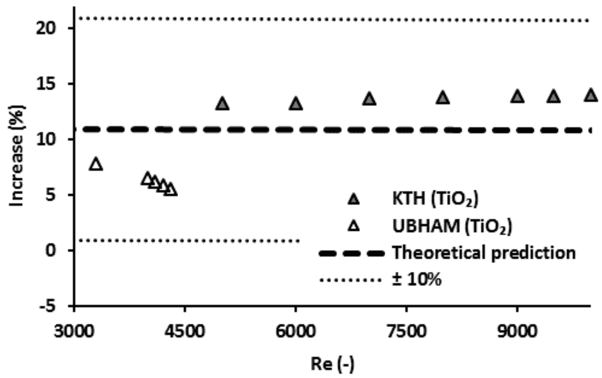
20
15
10
5
0
-5
Increase (%)
3000
4500
6000
7500
9000
Re (-)
KTH (TiO_2)
UBHAM (TiO_2)
Theoretical prediction
± 10%

(a)

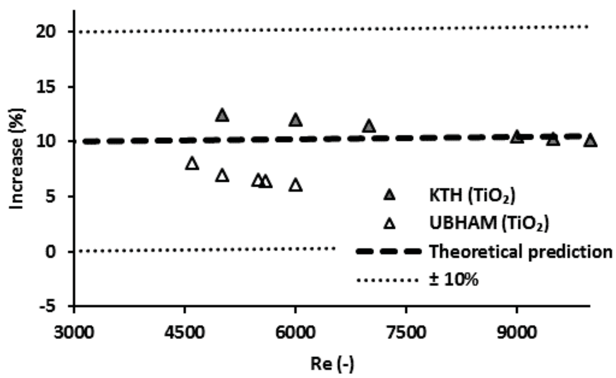
20
15
10
5
0
-5
Increase (%)
3000
4500
6000
7500
9000
Re (-)
KTH (TiO_2)
UBHAM (TiO_2)
Theoretical prediction
± 10%

(b)

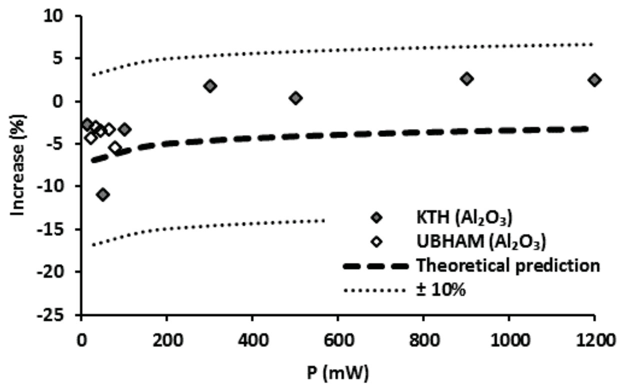

10
5
0
-5
-10
-15
-20
-25
Increase (%)
0
200
400
600
800
1000
1200
P (mW)
KTH (Al_2O_3)
UBHAM (Al_2O_3)
Theoretical prediction
± 10%

(a)

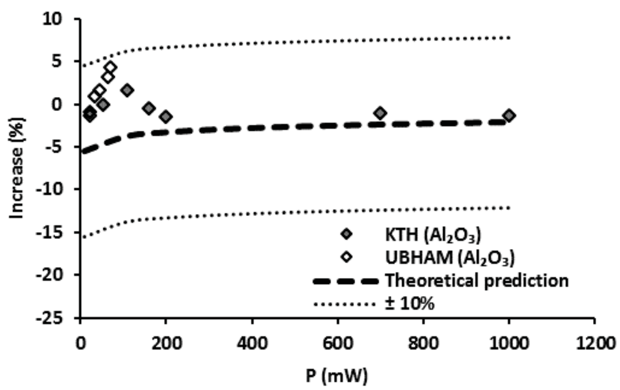

10
5
0
-5
-10
-15
-20
-25
Increase (%)
0
200
400
600
800
1000
1200
P (mW)
KTH (Al_2O_3)
UBHAM (Al_2O_3)
Theoretical prediction
± 10%

(b)

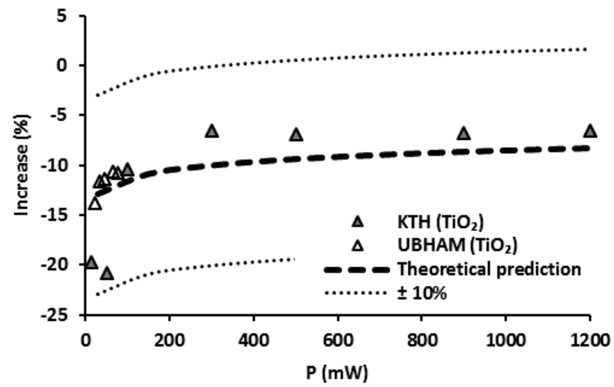

5
0
-5
-10
-15
-20
-25
Increase (%)
0
200
400
600
800
1000
1200
P (mW)
KTH (TiO2)
UBHAM (TiO2)
Theoretical prediction
± 10%

(a)

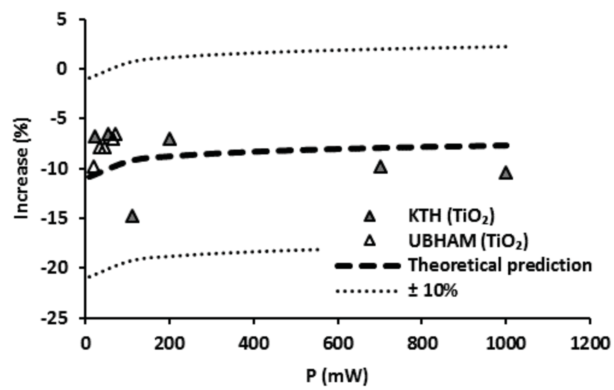

5
0
-5
-10
-15
-20
-25
Increase (%)
0
200
400
600
800
1000
1200
P (mW)
KTH (TiO2)
UBHAM (TiO2)
Theoretical prediction
± 10%

(b)

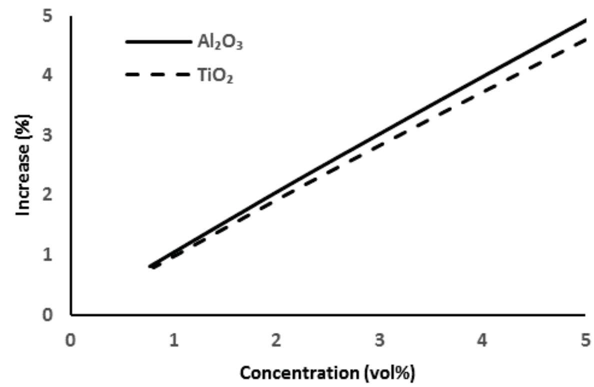
Al2O3
TiO2
Increase (%)
Concentration (vol%)
0
1
2
3
4
5

Highlights

- Turbulent heat transfer of nanofluids at similar conditions was investigated at two universities
- Nusselt numbers and friction factors in nanofluids can be predicted by single phase fluid correlations
- Comparison heat transfer coefficients of nanofluids and base fluids at equal Reynolds number is misleading
- This comparison at equal pumping power is an appropriate approach and takes into account the total cost of the system
- Based on the correct criterion this work show no benefit for cooling application with nanofluids in turbulent flow